CELL-2022-0055-ver9-Poveacabello_1P
Type: research-article

CELLULAR REPROGRAMMING
Volume 24, Number 0, 2022

DOI: 10.1089/cell.2022.0055

Research Article

Open camera or QR reader and scan code to access this article and other resources online.

Modeling Mitochondrial Encephalomyopathy, Lactic Acidosis, and Stroke-Like Episodes Syndrome Using Patient-Derived Induced Neurons Generated by Direct Reprogramming

Suleva Povea-Cabello,[1] Marina Villanueva-Paz,[2] Irene Villalón-García,[1] Marta Talaverón-Rey,[1] Mónica Álvarez-Cordoba,[1] Juan M. Suárez-Rivero,[1] María Ángeles Montes,[3] Antonio Rodríguez-Moreno,[4] Yuniesky Andrade-Talavera,[4] José A. Armengol,[3] and José A. Sánchez-Alcázar[1]

Abstract

Mitochondrial diseases are a heterogeneous group of rare genetic disorders caused by mutations in nuclear or mitochondrial DNA (mtDNA). These diseases are frequently multisystemic, although mainly affect tissues that require large amounts of energy such as the brain. Mutations in mitochondrial transfer RNA (mt-tRNA) lead to defects in protein translation that may compromise some or all mtDNA-encoded proteins. Mitochondrial Encephalomyopathy, Lactic Acidosis and Stroke-like episodes (MELAS) syndrome is mainly caused by the m.3243A>G mutation in the mt-tRNA$^{Leu(UUR)}$ (MT-TL1) gene. Owing to the lack of proper animal models, several cellular models have been developed to study the disease, providing insight in the pathophysiological mechanisms of MELAS. In this study, we show a successful direct conversion of MELAS patient-derived fibroblasts into induced neurons (iNs) for the first time, as well as an electrophysiological characterization of iNs cocultured with astrocytes. In addition, we performed bioenergetics analysis to study the consequences of m.3243A>G mutation in this neuronal model of MELAS syndrome.

Keywords: mitochondria, mitochondrial diseases, MELAS syndrome, direct reprogramming, induced neurons

Introduction

Mitochondrial diseases are rare genetic disorders caused by mutations in nuclear or mitochondrial DNA (mtDNA). Mutations in mtDNA are associated to several maternally inherited mitochondrial disorders. Mitochondrial Encephalomyopathy, Lactic Acidosis and Stroke-like episodes (MELAS) syndrome is one of the most prevalent ones. It is mainly caused by the m.3243A>G mutation in the mt-tRNA-$^{Leu(UUR)}$ (MT-TL1) gene (El-Hattab et al., 2015). This mutation affects the wobble position in the transfer RNA (tRNA), causing a defect in mitochondrial protein translation (King et al., 1992). MELAS m.3243A>G mutation is heteroplasmic, which means that mutant and wild-type (WT) mtDNA copies coexist within the same cell (El-Hattab et al., 2015).

MELAS is diagnosed according to the presence of specific phenotypic and genetic features (Finsterer, 2020; Yatsuga et al., 2012). MELAS syndrome is a multiorgan

[1]Centro Andaluz de Biología del Desarrollo (CABD-CSIC-Universidad Pablo de Olavide), and Centro de Investigación Biomédica en Red: Enfermedades Raras, Instituto de Salud Carlos III, Sevilla, Spain.
[2]Unidad de Gestión Clínica de Gastroenterología, Servicio de Farmacología Clínica, Instituto de Investigación Biomédica de Málaga-IBIMA, Hospital Universitario Virgen de la Victoria, Universidad de Málaga, Málaga, Spain.
[3]Departamento de Fisiología, Anatomía y Biología Celular, Universidad Pablo de Olavide, Sevilla, Spain.
[4]Laboratorio de Neurociencia Celular y Plasticidad, Departamento de Fisiología, Anatomía y Biología Celular, Universidad Pablo de Olavide, Sevilla, Spain.

disease, with wide manifestations such as stroke-like episodes, seizures, cortical vision loss, or diabetes (El-Hattab et al., 2015). Currently, there are no curative treatments for MELAS.

Owing to the lack of suitable animal models for this disease, several cellular models have been developed (Povea-Cabello et al., 2020). Fibroblasts derived from patients' biopsies have demonstrated to be a good model, since they manifest disease-related phenotypes, are easy to obtain and highly proliferative (Hu et al., 2019). However, the most affected tissues in this disease are the brain and the skeletal muscle, since they have higher energy requirements and mitochondrial density (DiMauro, 2007).

Reprogramming into induced pluripotent stem cells (iPSCs) and subsequent differentiation into neurons has been used for MELAS disease modeling (Hamalainen et al., 2013; Klein Gunnewiek et al., 2020; Kodaira et al., 2015), pharmacological screenings (Klein Gunnewiek et al., 2021), and gene therapy testing (Yang et al., 2018). However, this technique has several disadvantages. Reprogramming into iPSCs resets cellular age (Hsu et al., 2016), could cause mitochondrial rejuvenation and improvement of cell bioenergetics (Suhr et al., 2010). In addition, it causes a segregation of mtDNA and, after conversion, mutant and WT cells are obtained (Pickrell and Youle, 2013).

The first direct conversion of fibroblasts into induced neurons (iNs) was performed in 2010 (Vierbuchen et al., 2010), using a combination of proneural genes. Later, overexpression of additional genes and/or the use of microRNAs improved the technique (Pang et al., 2011; Yoo et al., 2011). Furthermore, a combination of small molecules and proneural growth factors that increase reprogramming efficiency was found (Ladewig et al., 2012; Pfisterer et al., 2016). Subsequently, the REST (repressor element-1 silencing transcription factor) complex, a barrier for adults fibroblasts reprogramming, was described and a single lentiviral vector for direct conversion of human adult fibroblasts into iNs was developed (Drouin-Ouellet et al., 2017).

The use of direct reprogramming techniques brings numerous advantages. First, the procedure is relatively simple and fast. In addition, unlike iPSCs, iNs maintain the age and the epigenetic marks of the donor (Drouin-Ouellet et al., 2017; Huh et al., 2016; Mertens et al., 2015). Furthermore, iNs maintain age-related mtDNA mutations (Wei et al., 2021) and are useful for studying mitochondrial aging (Kim et al., 2018). Moreover, neuronal cells obtained by direct conversion show less genome instability than those derived from iPSCs (Lee et al., 2019; Weissbein et al., 2014).

In this study, we show a successful direct conversion of MELAS patient-derived fibroblasts and we characterize the resulting iNs.

Materials and Methods

Reagents

Anti-TAU clone HT7, accutase, and fluorophore-conjugated secondary antibodies were from ThermoFisher Scientific; anti-microtubule-associated protein 2 (anti-MAP-2) from Abcam. LM-22A4, glial derivate neurotrophic factor (GDNF), neurotrophin-3 (NT-3), Noggin, and SB-431542 were purchased from R&D Systems; dibutyryl cAMP (db-cAMP), CHIR99021, LDN-193189, polyornithine, fibronectin, and laminin were from Sigma-Aldrich.

Fibroblasts cultures

Cultured fibroblasts were derived from a skin biopsy of a 44-year-old male MELAS patient harboring the heteroplasmic m.3243A>G mutation. Heteroplasmy load was determined by next-generation sequencing (NGS) using CleanPlex Mitochondrial Disease Panel (Paragon Genomics) and was found to be 75% in MELAS fibroblasts. Sequences of controls and MELAS fibroblasts are available at the Zenodo repository: https://doi.org/15281/zenodo.6610439 Heteroplasmy load did not change significantly during this study. Age and sex-matched control fibroblasts (39 and 48 years old) were derived from two healthy volunteers. Samples were obtained according to the Helsinki Declarations of 1964, as revised in 2001.

Generation of iNs by direct reprogramming of control and MELAS fibroblasts

Neurons were generated from patient and control fibroblasts by direct neuronal conversion as previously described (Drouin-Ouellet et al., 2017; Shrigley et al., 2018). Fibroblasts were plated onto 0.1% gelatin-coated T25 flasks or μ-Slide 4-Well Ibidi plates (2.6e4 cells/cm^2) with fibroblast ◀AU6 medium. On the following day, fibroblasts were transduced with the lentiviral vector containing neural lineage-specific transcription factors (Acsl1 and brain-2 [Brn2]) and two short hairpin RNA (shRNA) targeting REST complex. Transfer vector LV.U6.shREST1.U6.shREST2.hPGK.BRN2.hPGK.Ascl1.WPRE was a gift from Dr. Malin Parmar (Developmental and Regenerative Neurobiology, Lund University, Sweden). Transduction was performed at a multiplicity of infection of 30. The conversion was performed as previously described (Drouin-Ouellet et al., 2017; Shrigley et al., 2018).

Neuronal cells were identified by the expression of Tau and MAP-2. Conversion efficiency was calculated as the number of Tau$^+$ cells over the fibroblasts plated for conversion. Neuronal purity was calculated as the number of Tau$^+$ cells over the cells remaining in the plate after reprogramming. Whole well images were obtained with a CellDiscoverer7 microscope (Zeiss) fitted with an Axiocam 506 camera (10× magnification). 4′,6-Diamidino-2-phenylindole (DAPI)$^+$/Tau$^+$ cells were quantified using analyze particles from ImageJ software (NIH).

Measurement of mutant heteroplasmy

Heteroplasmy load was determined by Touch-Down polymerase chain reaction (PCR) and restriction fragment length polymorphism (RFLP) analysis. Genomic DNA extraction was performed using the Qiagen DNeasy Blood and tissue kit (Qiagen). To detect the A3243G MELAS mutation, DNA amplification was performed by using reverse primer 5′-AGGAATGCCATTGCGATTAG-3′ and forward primer 5′-CACTGTCAACCCAACACAGG-3′. After PCR, the amplicon was digested with *Apa*I (ThermoFisher) for 3 hours at 37°C.

For measuring iNs heteroplasmy, 27 days postinfection (DPI), cells were detached using accutase and they were seeded in culture plates coated with polyornithine (15 μg/mL), fibronectin (0.5 ng/μL), and laminin (5 μg/mL; hereinafter, PFL). The seeding of iNs in PFL-coated plates has been observed to increase the purity of the iNs culture up to 95% (Villanueva-Paz et al., 2019).

Electrophysiological recordings

iNs were cocultured with rat astrocytes to improve survival and ensure proper maturation. Rat astrocytes were obtained from dissection of P2 rats hippocampus. Astrocytes were cultured using Dulbecco's modified Eagle's medium (DMEM) Glutamax with 50 mg/mL penicillin/streptomycin and 10% fetal bovine serum. We used neuron-astrocytes ''sandwich'' coculture system as described (Jones et al., 2012). iNs were replated at 30 DPI and cocultured with astrocytes during 18–20 days before electrophysiological recordings. iNs were visually identified under an upright AU7 ▶ microscope using IR-DIC microscopy (Olympus) to perform whole single-cell patch-clamp recordings.

The coverslips were transferred to a submerged-type recording chamber, continuously perfused with standard artificial cerebrospinal fluid (ACSF) and allowed to stabilize at least 10 minutes before recordings being performed. ACSF containing (in mM) 124 NaCl, 2.69 KCl, 1.25 KH_2PO_4, 2 $MgSO_4$, 1.8 $CaCl_2$, 26 $NaHCO_3$, and 10 glucose (pH 7.2, 300 mOsm) was continuously bubbled with (5% CO_2, 95% O_2) and kept at 34°C throughout all recordings. Three to five cells per coverslip from at least three coverslips per group were recorded from for each iNs.

Passive electrophysiological membrane properties were measured immediately after access to the cell lumen was established in whole-cell patch-clamp mode. Recording borosilicate glass microelectrodes (5–7 MΩ) were filled with internal gluconate-based recording solution containing (in mM) 110 K+-gluconate, 40 HEPES, 4 NaCl, 4 ATP-Mg, and 0.3 GTP with pH set to 7.2–7.3 and osmolarity to 280–290 mOsmol/L. Resting membrane potential (RMP) was measured in current-clamp mode from 60-second-long recorded traces. To test the ability of the iNs to generate action potentials (AP) two different protocols were used in current-clamp mode: random delivered pulses through AU8 ▶ patch-pippete (2 nA, 5 mseconds) at RMP and step current pulses injected from −120 to +360 pA.

The occurrence of spontaneous synaptic activity was detected performing 60-second-long recordings in voltage-clamp mode holding the membrane at −70 mV. Recordings were performed with a patch-clamp amplifier (Multiclamp 700B) and data were acquired at 10 kHz, low-pass filtered at 1 kHz using pCLAMP 10.4 software (Molecular Devices) and digitized with a Digidata 1322A. Data were analyzed with the pCLAMP 10.4 software (Molecular Devices) and Sigmaplot 11. Normality was assessed with a Shapiro–Wilk test and Student's *t*-test, or Mann–Whitney tests were used for parametric or nonparametric distributed data, respectively. Only cells with an access resistance ranging from 10 to 30 MΩ were considered in the study and access resistance did not differ between control and MELAS recorded iNs (control: 19.4 ± 1.75 MΩ, $n = 14$; MELAS: 18.9 ± 1.67 MΩ, $n = 18$; $p = 0.860$, Student's *t*-test).

Bioenergetics analysis

Mitochondrial respiratory function of Control 1 and MELAS iNs was evaluated by Mito Stress test assay using a XFe24 extracellular flux analyzer (Seahorse Bioscience, Billerica, MA). Twenty-seven DPI, cells were replated onto PFL-coated XF24 cell culture plates (50,000 cells/well). Mito Stress Test protocol was followed as described (Divakaruni et al., 2014; Villanueva-Paz et al., 2019). Data were analyzed using the Seahorse Analytics platform (Agilent). The experiment was performed with more than five technical replicates.

Statistics

Results are expressed as mean ± standard deviation of three technical replicates. Differences were analyzed using Student's *t*-test with Welch correction.

Results

Direct conversion of control and MELAS fibroblasts into iNs

Neurons were generated from human fibroblasts derived from skin biopsies of healthy volunteers and a MELAS patient. For direct reprogramming, we followed the method described by Drouin-Ouellet et al. (2017) that uses a single lentiviral vector to express the proneural genes *Ascl1* and *Brn2* and silence REST complex (see Materials and Methods section). We monitored cellular morphological changes during the process by taking pictures as shown in Supplementary Figure S1. Twenty-seven DPI, cells exhibited a typical neuron-like morphology (Fig. 1A) and showed positive immunoreactivity against the neuronal markers Tau and MAP-2, which are microtubule-associated proteins (Fig. 1B). In contrast, those unconverted cells did not show Tau/MAP-2 staining. ◀ SF1 ◀ F1

Image analysis of controls and MELAS Tau^+ cells revealed the presence of elaborated neurites with bouton-like structures and/or spine-like protrusions at 27 DPI (Fig. 1C), suggesting iNs maturation.

Tau^+ cells were used to evaluate conversion efficiency and neuronal purity (Fig. 2A). Conversion efficiency was 38% in Control 1 (38% ± 8%), 31% in Control 2 (31% ± 7%), and 32% in MELAS (32% ± 3%) cells (Fig. 2B), and neuronal purity was 65% (65% ± 9%) in Control 1, 76% (76% ± 10%) in Control 2, and up to 80% (79% ± 10%) in MELAS cells (Fig. 2C). There were not statistically significant differences between controls and MELAS conversion efficiency and purity. ◀ F2

Maintenance of heteroplasmy levels after direct reprogramming

We examined whether levels of m.3243A>G mutation were affected by direct reprogramming. Skin fibroblasts derived from a MELAS patient harboring the m.3243A>G mutation were used for direct reprogramming. The mutational load was quantified by NGS resulting in 75% (Fig. 2D). Heteroplasmy loads were continuously followed up to exclude potential changes in the percentage of mutated mtDNA.

Then, we compared m.3243A>G heteroplasmy levels between both patient-derived fibroblasts and the iNs generated. Twenty-seven DPI and before DNA extraction, controls and MELAS iNs were seeded onto PFL-coated plates to enrich the population of neurons. We checked the levels of m.3243A>G mutation by RFLP-PCR and they closely reflected those of the corresponding primary fibroblasts (Fig. 2D). Therefore, we concluded that m.3243A>G proportions did not significantly change during direct reprogramming. Representative gel images for both fibroblasts and iNs are shown in Supplementary Figure S2. ◀ SF2

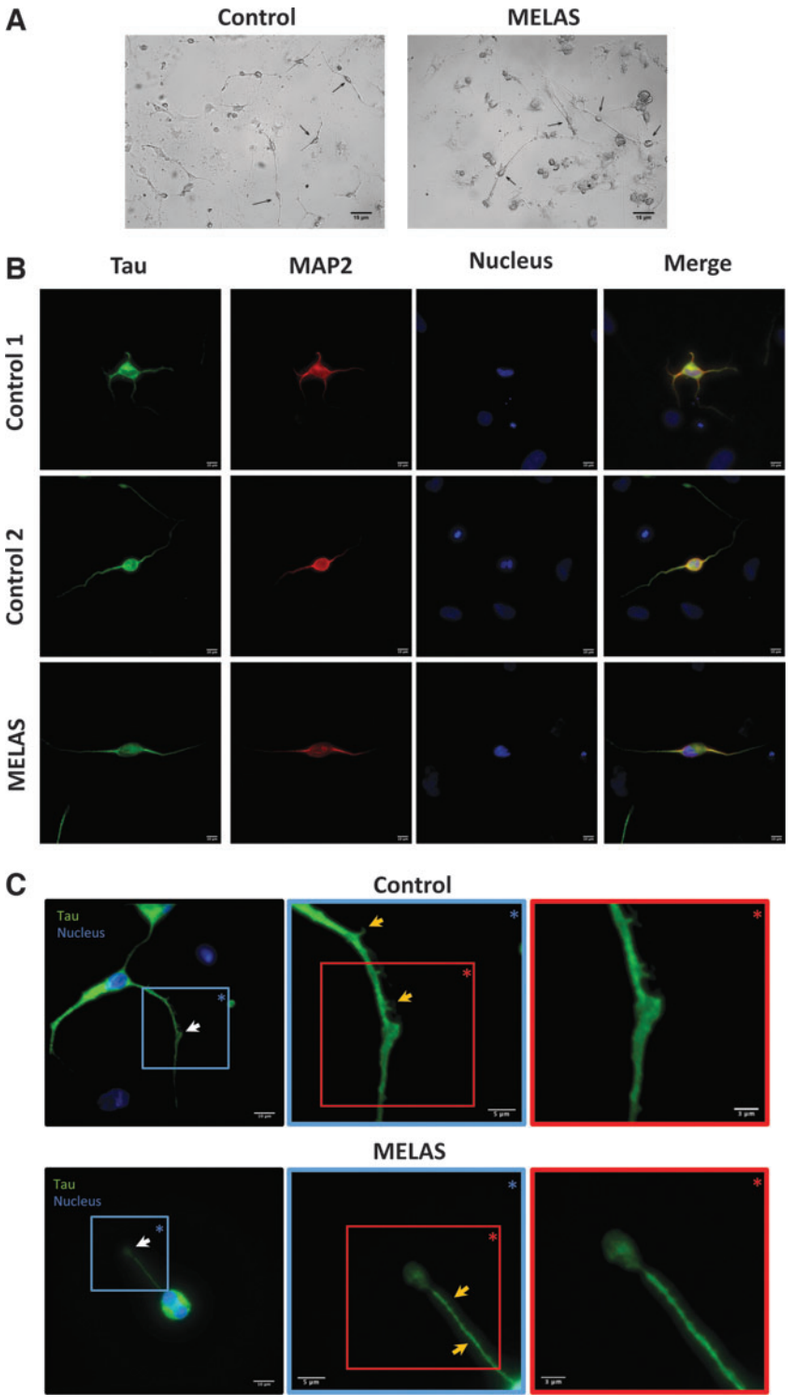

AU13 ▶ **FIG. 1.** Generation of iNs from controls and MELAS fibroblasts. **(A)** Direct reprogramming was stopped 27 DPI and cells exhibited a neuronal morphology (*black arrows*). Pictures were taken using a brightfield microscope (Leica DMi1; Leica Microsystems GmbH, Wetzlar, Germany). Scale bar = 15 μm. **(B)** Immunofluorescence staining of control and MELAS iNs. Cells were immunostained for the neuronal markers Tau and MAP-2. DAPI was used to stain cell nuclei (in *blue*). Scale bar = 10 μm. **(C)** Morphological observation of control and MELAS iNs. After direct reprogramming, cells exhibited morphological features such as spine-like protrusions and bouton-like structures, suggesting
4C ▶ neuronal maturation. DAPI, 4′,6-diamidino-2-phenylindole; DPI, days postinfection; iNs, induced neurons; MAP-2, microtubule-associated protein 2; MELAS, Mitochondrial Encephalomyopathy, Lactic Acidosis and Stroke-like episodes.

Electrophysiological recordings of control and MELAS iNs

Control and MELAS iNs were cocultured with rat astrocytes in a ''sandwich'' coculture system described by Jones
F3 ▶ et al. (2012) as shown in Figure 3A. Both control and MELAS iNs showed low capacity of burst firing in response to sustained depolarizing current injections, with some cells firing only one AP at the onset of the depolarization and a prominent sag to hyperpolarizing current steps (Fig. 3B). However, both groups showed ability to generate APs in response to random short depolarizing pulses (control: 33.3% and MELAS: 38.9% of the total recorded cells; Fig. 3B). Interestingly, control group showed a larger ratio of cells displaying spontaneous activity compared with MELAS iNs (control: 26.7% and MELAS: 22.2% of the total recorded cells; Fig. 3C).

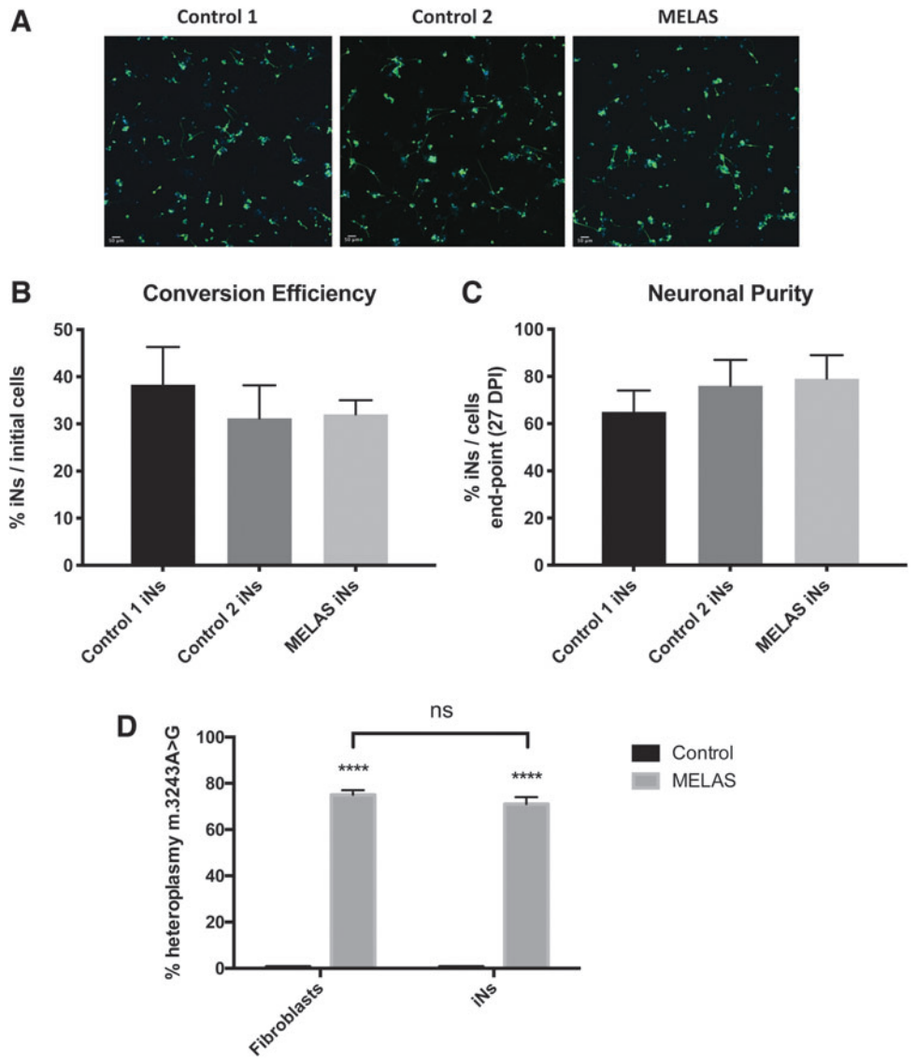

FIG. 2. Characterization of controls and MELAS iNs. **(A)** Tau immunostaining was used to calculate the conversion efficiency and the neuronal purity, and the results are plotted in **(B**, **C)**. The data are shown in the graphs as the mean ± SD of three technical replicates. **(D)** Heteroplasmy load in MELAS fibroblasts and iNs derived from them. Heteroplasmy loads were determined by PCR-RFLP assay. Results are expressed as the mean ± SD of three biological replicates. Significance of MELAS with respect to controls fibroblasts or iNs was represented as ****$p < 0.0001$. There were no statistically significant differences (ns) between fibroblasts and iNs heteroplasmy loads. PCR, polymerase chain reaction; RFLP, restriction fragment length polymorphism; SD, standard deviation. ◀4C

Moreover, MELAS iNs showed a lower membrane capacitance (Cm) compared with control (control: 17.6 ± 3.31 pF, $n = 14$, MELAS: 8.56 ± 0.87 pF, $n = 18$; $p = 0.002$ Mann–Whitney rank sum test, Fig. 3D**),** which is also accompanied by a decreased time constant (control: 308.7 ± 40.5 μseconds, $n = 13$, MELAS: 185.7 ± 37.6 μseconds, $n = 18$; $p = 0.013$ Mann–Whitney rank sum test, Fig. 3E). In addition, we did not observe differences in the RMP between both groups (control: −32.3 ± 3.35 mV, $n = 14$, MELAS: −31.2 ± 1.67 mV, $n = 18$; $p = 0.765$ Student's t-test, Fig. 3F) and the control group showed smaller membrane resistance (Rm; control: 1674.4 ± 558.1 MΩ, $n = 14$, MELAS: 2062.3 ± 227.6 MΩ, $n = 18$; $p = 0.030$ Mann–Whitney rank sum test, Fig. 3G).

MELAS iNs show alterations in mitochondrial bioenergetics

To evaluate cellular bioenergetics, Control and MELAS iNs were plated onto PFL-coated Seahorse XFe24 plates and the Mito Stress test was performed.

The respiratory profile of control and MELAS iNs are shown in Figure 4A. Oxygen consumption rate data were ◀F4 used to calculate key parameters such as basal respiration, maximal respiration, spare respiratory capacity, and ATP-linked respiration (Fig. 4B–E). All parameters were reduced in MELAS iNs in comparison with controls. This assay demonstrated that MELAS iNs have a decreased mitochondrial function and confirms that m.3243A>G mutation leads to alterations in mitochondrial respiration in iNs model of MELAS syndrome.

Discussion

In this study, we have successfully generated disease-specific iNs by direct reprogramming of MELAS patient-derived fibroblasts harboring the m.3243A>G mutation for the first time.

Reprogramming efficiency, which is the percentage of iNs over the fibroblasts plated for conversion, was ∼35% in both control and MELAS cells. High heteroplasmy loads, such as 75% in the parental MELAS fibroblasts, did not

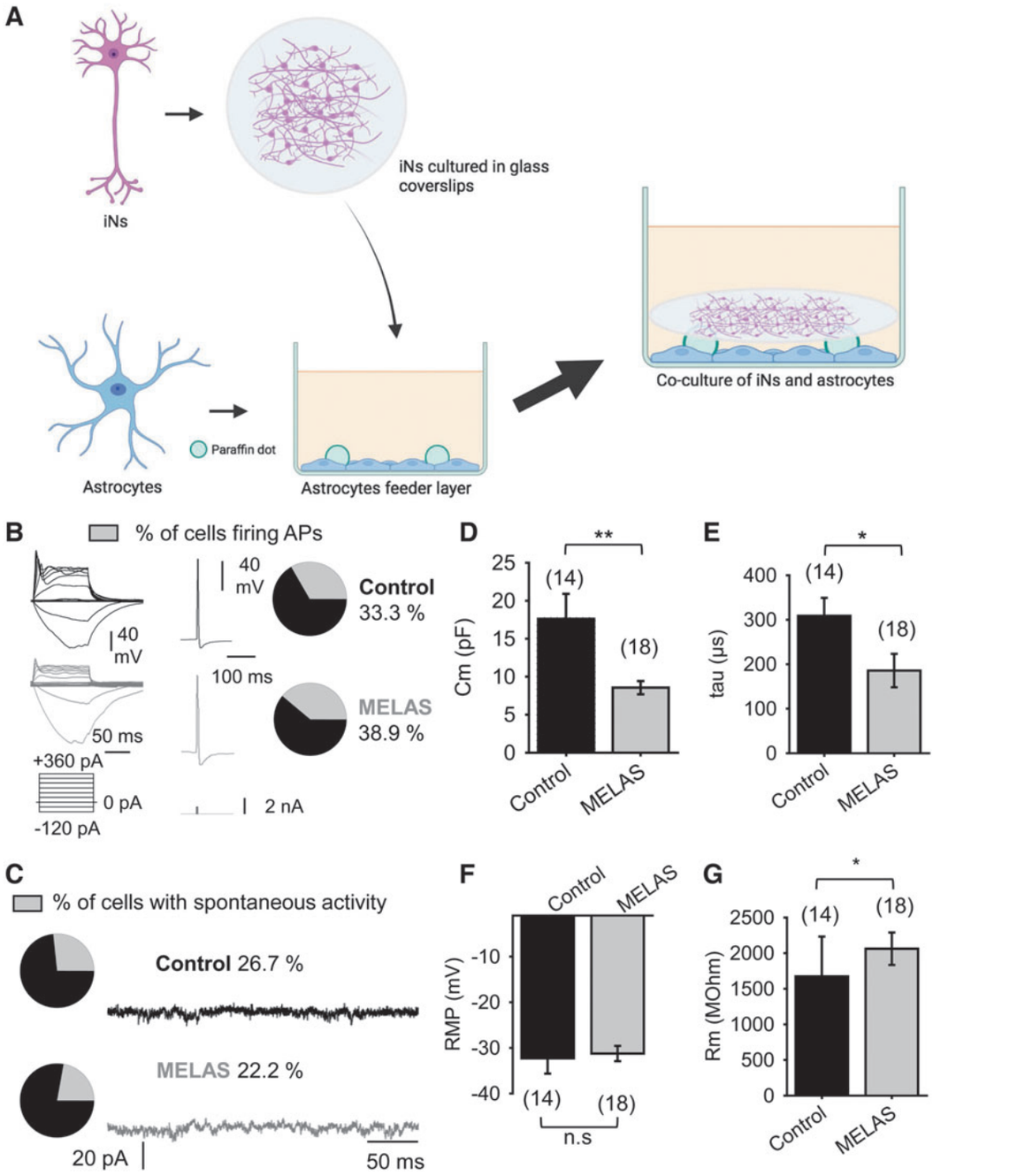

FIG. 3. Electrophysiological characterization of control and MELAS iNs after coculture with astrocytes. **(A)** After conversion, iNs were plated onto PFL-coated glass coverslips and astrocytes were seeded onto 4-well plates with paraffin dots. When confluent, iNs coverslips were transferred to astrocytes wells and cocultured during 18–20 days in late neuronal medium. **(B)** Representative sample traces of iNs from control (*black*) and MELAS (*gray*) responses to depolarizing current steps (*left*) and random depolarizing pulses stimulation (*right*). Stimulation pattern is shown at the *bottom* for each corresponding protocol and the ratio of firing cells is shown in *gray* in the pie charts on the *right panels* as the percentage of firing cells out of total recorded cells. **(C)** Representative sample traces (*right*) recorded in voltage-clamp configuration (−70 mV hold) from control (*black*) and MELAS iNs (*gray*). *Left*: The ratio of cells displaying spontaneous activity is shown in *gray* in the pie charts as a percentage out of the total recorded cells. **(D–G)** Summary of the membrane capacitance, membrane time constant, resting membrane potential and membrane resistance, respectively, for control (*black*) and MELAS (*gray*) iNs. Data are presented as mean ± SEM. Significance is set as $*p < 0.05$, $**p < 0.01$. SEM, standard error of the mean.

4C ▶

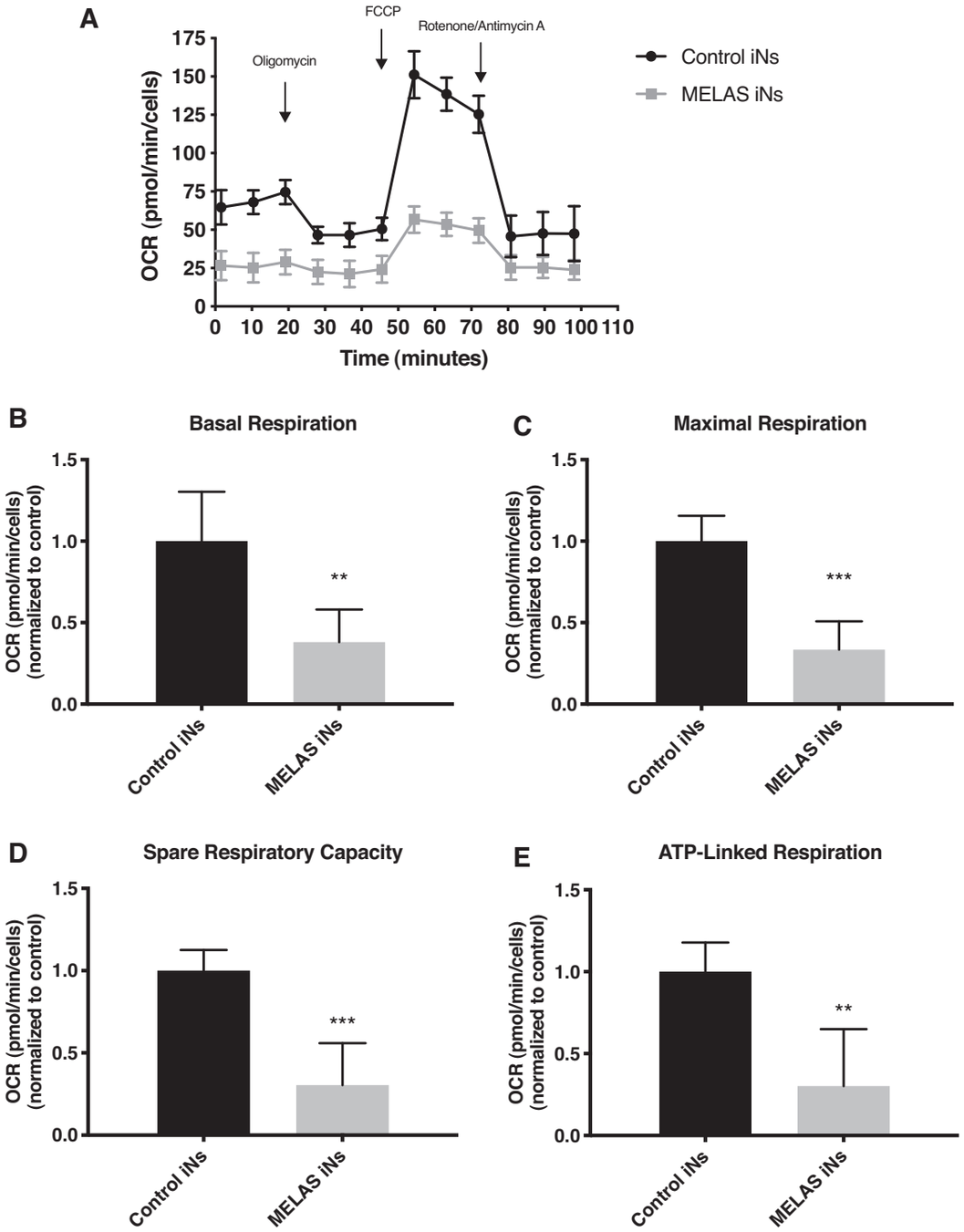

FIG. 4. Control and MELAS iNs respiratory profile. **(A)** Oxygen consumption rate of Control 1 and MELAS iNs was measured under basal conditions followed by the sequential addition of oligomycin, FCCP and rotenone and antimycin A using a Seahorse Extracellular Flux Analyzer. Parameters of respiratory profile of control and MELAS iNs are plotted in **(B)** basal respiration, **(C)** maximal respiration, **(D)** spare respiratory capacity, and **(E)** ATP-linked respiration. Results are expressed as mean ± SD of more than five technical replicates in both control and MELAS iNs. Significance of MELAS with respect to control iNs is represented as $^{**}p < 0.01$, $^{***}p < 0.001$. All OCR measurements were normalized to cell number. OCR, oxygen consumption rate.

compromise conversion efficiency. We found no differences between control and MELAS cells, which is in line with our previous work in Myoclonic Epilepsy with Ragged-Red Fibers (MERRF) syndrome (Villanueva-Paz et al., 2019, 2020) and Drouin-Ouellet's et al. (2017) work in Parkinson's, Huntington's, and Alzheimer's disease. In our case, we found no significant difference between controls conversion efficiencies, although variability can occur, especially if they differ in age and sex.

Another important parameter is neuronal purity, which is the percentage of iNs after conversion and determines the homogeneity of the culture. In our case, we reached high culture purity in control and MELAS iNs, being approximately a 70%–80%, and we found no significant differences between them. In other work from our group, in which we converted MERRF fibroblasts into iNs (Villanueva-Paz et al., 2019), we did observe differences between diseased and controls cells. However, variability among mitochondrial diseases patients and MELAS syndrome phenotypic complexity could explain why we did not observe those differences.

In this study, indicators of neuronal maturation such as bouton-like structures and spine-like protrusions were observed in both control and MELAS iNs. This is in line with our studies in MERRF iNs, in which we also observed elaborate neurites (Villanueva-Paz et al., 2019).

Heteroplasmy maintenance is crucial if iNs are going to be used for patient-specific disease modeling or personalized medicine. When using m.3243A>G MELAS fibroblasts for conversion into iPSCs, high heteroplasmy and WT lines are obtained (Hamalainen et al., 2013; Kodaira et al., 2015) and, consequently, iPSCs-derived neurons are not suitable for personalized approaches. Direct reprogramming overcomes this drawback since, as we demonstrated in previous studies, iNs maintain the heteroplasmy load of the parental fibroblasts (Villanueva-Paz et al., 2019). In this study, we did not observe differences between MELAS iNs and fibroblasts' heteroplasmy load determined by RFLP-PCR, suggesting that these iNs are suitable for disease modeling and personalized medicine. However, NGS experiments should be performed to precisely verify that heteroplasmy levels are not affected.

Electrophysiological recordings of iNs generated by direct conversion have shown that they acquire neuronal functional properties alone or cocultured with glia between 85 and 100 DPI (Drouin-Ouellet et al., 2017; Villanueva-Paz et al., 2020). In this study, to promote neuronal maturation, we cocultured iNs with rat astrocytes. Control and MELAS iNs showed electrophysiological properties and, interestingly, the ratio of cells with spontaneous activity was higher in the control group, suggesting that control iNs display more functional ability to establish synaptic contacts and/or release neurotransmitters to the medium.

This is in line with a previous work in MELAS iPSCs-derived neurons (Klein Gunnewiek et al., 2020), in which frequency of spontaneous excitatory activity was reduced in cells with high m.3243A>G heteroplasmy. Electrophysiological recordings of iNs at longer postinduction time points should be performed to elucidate whether more mature stages emerge and whether more functional differences between control and MELAS exist when iNs get older.

The m.3243A>G mutation has demonstrated to reduce mitochondrial respiration in cellular models of MELAS syndrome such as fibroblasts (Lin et al., 2017). In our study, we found that mitochondrial respiratory profile was decreased in MELAS iNs in comparison with Control 1 iNs. In concrete, MELAS iNs showed a decreased basal, maximal, and ATP-linked respiration as well as spare respiratory capacity. A decreased mitochondrial function in MELAS cells indicates the impairment of oxidative phosphorylation (OXPHOS), which is consistent with the ETC complexes deficiency caused by the A3243G mutation (King et al., 1992). Moreover, our findings are in line with a recent study showing significant low levels of mitochondrial function in MELAS iPSCs-derived neurons (Klein Gunnewiek et al., 2020). However, more studies are needed to determine the pathophysiological consequences of m.3243A>G mutation in iNs cultures.

Conclusion

This study demonstrates that MELAS iNs harboring the m.3243A>G mutation can be successfully generated from patient-derived fibroblasts. These iNs maintain the heteroplasmy load of the fibroblasts and, cocultured with astrocytes, show electrophysiological properties. In addition, MELAS iNs exhibit pathophysiological features such as decreased bioenergetics. Therefore, direct reprogramming is a promising strategy for mitochondrial disease studies and pharmacological screening.

Authors' Contributions

S.P.-C., M.V.-P., and J.A.S.-A. designed, directed, and wrote the study. S.P.-C. performed the direct reprograming. S.P.-C., I.V.-G., and M.T.-R. performed the plasmids and viruses production. J.M.S.-R. and M.A.-C. maintained cell cultures. J.A.A. and M.A.M. obtained astrocytes for cocultures. A.R.-M. and Y.A.-T. performed the electrophysiological assays and analyzed data.

Acknowledgments

We thank Dr. Malin Parmar's group (Developmental and Regenerative Neurobiology, Lund University, Sweden) for the plasmids used for reprogramming. We thank Dr. Janelle Drouin-Ouellet's group (Faculty of Pharmacy. University of Montreal, Quebec, Canada) for training and advise in direct reprogramming and disease modeling in iNs. The supports of ''Ayudas para Estancias Breves para beneficiarios FPU,'' AEPMI Association, ASANOL Association, Fúndación Mencia, Fundación Antonio Guerrero, FEDER (Federación Española de Enfermedades Raras), Yo Nemálínica Association, KAT6A Association, Superauténticos Association, Fundación MERCK Salud and Fundación MEHUER/ Colegio Oficial de Farmacéuticos de Sevilla are gratefully acknowledged.

Author Disclosure Statement ◀AU9

The authors declare they have no conflicting financial interests.

Funding Information ◀AU10

This study was supported by FIS PI16/00786 and PI19/00377 grants, Ministerio de Sanidad, Spain and Fondo

Europeo de Desarrollo Regional (FEDER-Unión Europea), Spanish Ministry of Education, Culture and Sport, ''Ayudas para la Formación de Profesorado Universitario'' (FPU) and Proyectos de Investigación de Excelencia de la Junta de Andalucía CTS-5725 and PY18-850. M.V.-P. holds a Sara Borrell (CD21/00198) research contract from ISCIII and Consejería de Salud de Andalucía.

Supplementary Material

Supplementary Figure S1
Supplementary Figure S2

AU11 ► **References**

Chinnery, P.F. (2015). Mitochondrial disease in adults: what's old and what's new? EMBO Mol. Med. 7, 1503–1512.

DiMauro, S. (2007). Mitochondrial DNA medicine. Biosci. Rep. 27, 5–9.

Divakaruni, A.S., Paradyse, A., Ferrick, D.A., Murphy, A.N., and Jastroch, M. (2014). Analysis and interpretation of microplate-based oxygen consumption and pH data. Methods Enzymol. 547, 309–354.

Drouin-Ouellet, J., Lau, S., Brattas, P.L., Rylander Ottosson, D., Pircs, K., Grassi, D.A., Collins, L.M., Vuono, R., Andersson Sjoland, A., Westergren-Thorsson, G., Graff, C., Minthon, L., Toresson, H., Barker, R.A., Jakobsson, J., and Parmar, M. (2017). REST suppression mediates neural conversion of adult human fibroblasts via microRNA-dependent and -independent pathways. EMBO Mol. Med. 9, 1117–1131.

El-Hattab, A.W., Adesina, A.M., Jones, J., and Scaglia, F. (2015). MELAS syndrome: clinical manifestations, pathogenesis, and treatment options. Mol. Genet. Metab. 116, 4–12.

El-Hattab, A.W., Hsu, J.W., Emrick, L.T., Wong, L.J., Craigen, W.J., Jahoor, F., and Scaglia, F. (2012). Restoration of impaired nitric oxide production in MELAS syndrome with citrulline and arginine supplementation. Mol. Genet. Metab. 105, 607–614.

Finsterer, J. (2020). Rare phenotypic manifestations of MELAS. Yonsei Med. J. 61, 904–906.

Glover, E.I., Martin, J., Maher, A., Thornhill, R.E., Moran, G.R., and Tarnopolsky, M.A. (2010). A randomized trial of coenzyme Q10 in mitochondrial disorders. Muscle Nerve 42, 739–748.

Gorman, G.S., Chinnery, P.F., DiMauro, S., Hirano, M., Koga, Y., McFarland, R., Suomalainen, A., Thorburn, D.R., Zeviani, M., and Turnbull, D.M. (2016). Mitochondrial diseases. Nat. Rev. Dis. Primers 2, 16080.

Hamalainen, R.H. (2014). Induced pluripotent stem cell-derived models for mtDNA diseases. Methods Enzymol. 547, 399–415.

Hamalainen, R.H., Manninen, T., Koivumaki, H., Kislin, M., Otonkoski, T., and Suomalainen, A. (2013). Tissue- and cell-type-specific manifestations of heteroplasmic mtDNA 3243A>G mutation in human induced pluripotent stem cell-derived disease model. Proc. Natl. Acad. Sci. U. S. A. 110, E3622–E3630.

Hsu, Y.C., Chen, C.T., and Wei, Y.H. (2016). Mitochondrial resetting and metabolic reprogramming in induced pluripotent stem cells and mitochondrial disease modeling. Biochim. Biophys. Acta 1860, 686–693.

Hu, S.Y., Zhuang, Q.Q., Qiu, Y., Zhu, X.F., and Yan, Q.F. (2019). Cell models and drug discovery for mitochondrial diseases. J. Zhejiang Univ. Sci. B 20, 449–456.

Huh, C.J., Zhang, B., Victor, M.B., Dahiya, S., Batista, L.F., Horvath, S., and Yoo, A.S. (2016). Maintenance of age in human neurons generated by microRNA-based neuronal conversion of fibroblasts. Elife. 5:e18648.

Inak, G., Lorenz, C., Lisowski, P., Zink, A., Mlody, B., and Prigione, A. (2017). Concise review: induced pluripotent stem cell-based drug discovery for mitochondrial disease. Stem Cells 35, 1655–1662.

Jones, E.V., Cook, D., and Murai, K.K. (2012). A neuron-astrocyte co-culture system to investigate astrocyte-secreted factors in mouse neuronal development. Methods Mol. Biol. 814, 341–352.

Kang, E., Wang, X., Tippner-Hedges, R., Ma, H., Folmes, C.D., Gutierrez, N.M., Lee, Y., Van Dyken, C., Ahmed, R., Li, Y., Koski, A., Hayama, T., Luo, S., Harding, C.O., Amato, P., Jensen, J., Battaglia, D., Lee, D., Wu, D., Terzic, A., Wolf, D.P., Huang, T., and Mitalipov, S. (2016). Age-related accumulation of somatic mitochondrial DNA mutations in adult-derived human iPSCs. Cell Stem Cell 18, 625–636.

Kim, Y., Zheng, X., Ansari, Z., Bunnell, M.C., Herdy, J.R., Traxler, L., Lee, H., Paquola, A.C.M., Blithikioti, C., Ku, M., Schlachetzki, J.C.M., Winkler, J., Edenhofer, F., Glass, C.K., Paucar, A.A., Jaeger, B.N., Pham, S., Boyer, L., Campbell, B.C., Hunter, T., Mertens, J., and Gage, F.H. (2018). Mitochondrial aging defects emerge in directly reprogrammed human neurons due to their metabolic profile. Cell Rep. 23, 2550–2558.

King, M.P., Koga, Y., Davidson, M., and Schon, E.A. (1992). Defects in mitochondrial protein synthesis and respiratory chain activity segregate with the tRNA(Leu(UUR)) mutation associated with mitochondrial myopathy, encephalopathy, lactic acidosis, and strokelike episodes. Mol. Cell. Biol. 12, 480–490.

Klein Gunnewiek, T.M., Van Hugte, E.J.H., Frega, M., Guardia, G.S., Foreman, K., Panneman, D., Mossink, B., Linda, K., Keller, J.M., Schubert, D., Cassiman, D., Rodenburg, R., Vidal Folch, N., Oglesbee, D., Perales-Clemente, E., Nelson, T.J., Morava, E., Nadif Kasri, N., and Kozicz, T. (2020). m.3243A > G-induced mitochondrial dysfunction impairs human neuronal development and reduces neuronal network activity and synchronicity. Cell Rep. 31, 107538.

Klein Gunnewiek, T.M., Verboven, A.H.A., Pelgrim, I., Hogeweg, M., Schoenmaker, C., Renkema, H., Beyrath, J., Smeitink, J., de Vries, B.B.A., Hoen, P.A.C., Kozicz, T., and Nadif Kasri, N. (2021). Sonlicromanol improves neuronal network dysfunction and transcriptome changes linked to m.3243A>G heteroplasmy in iPSC-derived neurons. Stem Cell Reports 16, 2197–2212.

Kodaira, M., Hatakeyama, H., Yuasa, S., Seki, T., Egashira, T., Tohyama, S., Kuroda, Y., Tanaka, A., Okata, S., Hashimoto, H., Kusumoto, D., Kunitomi, A., Takei, M., Kashimura, S., Suzuki, T., Yozu, G., Shimojima, M., Motoda, C., Hayashiji, N., Saito, Y., Goto, Y., and Fukuda, K. (2015). Impaired respiratory function in MELAS-induced pluripotent stem cells with high heteroplasmy levels. FEBS Open Bio 5, 219–225.

Ladewig, J., Mertens, J., Kesavan, J., Doerr, J., Poppe, D., Glaue, F., Herms, S., Wernet, P., Kogler, G., Muller, F.J., Koch, P., and Brustle, O. (2012). Small molecules enable highly efficient neuronal conversion of human fibroblasts. Nat. Methods 9, 575–578.

Lee, M., Sim, H., Ahn, H., Ha, J., Baek, A., Jeon, Y.J., Son, M.Y., and Kim, J. (2019). Direct reprogramming to human induced neuronal progenitors from fibroblasts of familial and sporadic Parkinson's disease patients. Int. J. Stem Cells 12, 474–483.

Lekoubou, A., Kouame-Assouan, A.E., Cho, T.H., Luaute, J., Nighoghossian, N., and Derex, L. (2011). Effect of long-term oral treatment with L-arginine and idebenone on the prevention of stroke-like episodes in an adult MELAS patient. Rev. Neurol. (Paris) 167, 852–855.

Lin, D.S., Kao, S.H., Ho, C.S., Wei, Y.H., Hung, P.L., Hsu, M.H., Wu, T.Y., Wang, T.J., Jian, Y.R., Lee, T.H., and Chiang, M.F. (2017). Inflexibility of AMPK-mediated metabolic reprogramming in mitochondrial disease. Oncotarget 8, 73627–73639.

Lorenz, C., Lesimple, P., Bukowiecki, R., Zink, A., Inak, G., Mlody, B., Singh, M., Semtner, M., Mah, N., Aure, K., Leong, M., Zabiegalov, O., Lyras, E.M., Pfiffer, V., Fauler, B., Eichhorst, J., Wiesner, B., Huebner, N., Priller, J., Mielke, T., Meierhofer, D., Izsvak, Z., Meier, J.C., Bouillaud, F., Adjaye, J., Schuelke, M., Wanker, E.E., Lombes, A., and Prigione, A. (2017). Human iPSC-derived neural progenitors are an effective drug discovery model for neurological mtDNA disorders. Cell Stem Cell 20, 659.e9–674.e9.

Mertens, J., Paquola, A.C.M., Ku, M., Hatch, E., Bohnke, L., Ladjevardi, S., McGrath, S., Campbell, B., Lee, H., Herdy, J.R., Goncalves, J.T., Toda, T., Kim, Y., Winkler, J., Yao, J., Hetzer, M.W., and Gage, F.H. (2015). Directly reprogrammed human neurons retain aging-associated transcriptomic signatures and reveal age-related nucleocytoplasmic defects. Cell Stem Cell 17, 705–718.

Ohsawa, Y., Hagiwara, H., Nishimatsu, S.I., Hirakawa, A., Kamimura, N., Ohtsubo, H., Fukai, Y., Murakami, T., Koga, Y., Goto, Y.I., Ohta, S., and Sunada, Y.; KN01 Study Group. (2019). Taurine supplementation for prevention of stroke-like episodes in MELAS: a multicentre, open-label, 52-week phase III trial. J. Neurol. Neurosurg. Psychiatry 90, 529–536.

Pang, Z.P., Yang, N., Vierbuchen, T., Ostermeier, A., Fuentes, D.R., Yang, T.Q., Citri, A., Sebastiano, V., Marro, S., Sudhof, T.C., and Wernig, M. (2011). Induction of human neuronal cells by defined transcription factors. Nature 476, 220–223.

Perales-Clemente, E., Cook, A.N., Evans, J.M., Roellinger, S., Secreto, F., Emmanuele, V., Oglesbee, D., Mootha, V.K., Hirano, M., Schon, E.A., Terzic, A., and Nelson, T.J. (2016). Natural underlying mtDNA heteroplasmy as a potential source of intra-person hiPSC variability. EMBO J. 35, 1979–1990.

Pfisterer, U., Ek, F., Lang, S., Soneji, S., Olsson, R., and Parmar, M. (2016). Small molecules increase direct neural conversion of human fibroblasts. Sci. Rep. 6, 38290.

Pickrell, A.M., and Youle, R.J. (2013). Mitochondrial disease: mtDNA and protein segregation mysteries in iPSCs. Curr. Biol. 23, R1052–R1054.

Povea-Cabello, S., Villanueva-Paz, M., Suarez-Rivero, J.M., Alvarez-Cordoba, M., Villalon-Garcia, I., Talaveron-Rey, M., Suarez-Carrillo, A., Munuera-Cabeza, M., and Sanchez-Alcazar, J.A. (2020). Advances in mt-tRNA mutation-caused mitochondrial disease modeling: patients' brain in a dish. Front. Genet. 11, 610764.

Schon, E.A., DiMauro, S., and Hirano, M. (2012). Human mitochondrial DNA: roles of inherited and somatic mutations. Nat. Rev. Genet. 13, 878–890.

Shrigley, S., Pircs, K., Barker, R.A., Parmar, M., and Drouin-Ouellet, J. (2018). Simple generation of a high yield culture of induced neurons from human adult skin fibroblasts. J. Vis. Exp. 56904.

Smith, C., Abalde-Atristain, L., He, C., Brodsky, B.R., Braunstein, E.M., Chaudhari, P., Jang, Y.Y., Cheng, L., and Ye, Z. (2015). Efficient and allele-specific genome editing of disease loci in human iPSCs. Mol. Ther. 23, 570–577.

Suhr, S.T., Chang, E.A., Tjong, J., Alcasid, N., Perkins, G.A., Goissis, M.D., Ellisman, M.H., Perez, G.I., and Cibelli, J.B. (2010). Mitochondrial rejuvenation after induced pluripotency. PLoS One 5, e14095.

Vierbuchen, T., Ostermeier, A., Pang, Z.P., Kokubu, Y., Sudhof, T.C., and Wernig, M. (2010). Direct conversion of fibroblasts to functional neurons by defined factors. Nature 463, 1035–1041.

Villanueva-Paz, M., Povea-Cabello, S., Villalon-Garcia, I., Alvarez-Cordoba, M., Suarez-Rivero, J.M., Talaveron-Rey, M., Jackson, S., Falcon-Moya, R., Rodriguez-Moreno, A., and Sanchez-Alcazar, J.A. (2020). Parkin-mediated mitophagy and autophagy flux disruption in cellular models of MERRF syndrome. Biochim. Biophys. Acta Mol. Basis Dis. 1866, 165726.

Villanueva-Paz, M., Povea-Cabello, S., Villalon-Garcia, I., Suarez-Rivero, J.M., Alvarez-Cordoba, M., de la Mata, M., Talaveron-Rey, M., Jackson, S., and Sanchez-Alcazar, J.A. (2019). Pathophysiological characterization of MERRF patient-specific induced neurons generated by direct reprogramming. Biochim. Biophys. Acta Mol. Cell Res. 1866, 861–881.

Wei, W., Gaffney, D.J., and Chinnery, P.F. (2021). Cell reprogramming shapes the mitochondrial DNA landscape. Nat. Commun. 12, 5241.

Weissbein, U., Ben-David, U., and Benvenisty, N. (2014). Virtual karyotyping reveals greater chromosomal stability in neural cells derived by transdifferentiation than those from stem cells. Cell Stem Cell 15, 687–691.

Yang, Y., Wu, H., Kang, X., Liang, Y., Lan, T., Li, T., Tan, T., Peng, J., Zhang, Q., An, G., Liu, Y., Yu, Q., Ma, Z., Lian, Y., Soh, B.S., Chen, Q., Liu, P., Chen, Y., Sun, X., Li, R., Zhen, X., Liu, P., Yu, Y., Li, X., and Fan, Y. (2018). Targeted elimination of mutant mitochondrial DNA in MELAS-iPSCs by mitoTALENs. Protein Cell 9, 283–297.

Yatsuga, S., Povalko, N., Nishioka, J., Katayama, K., Kakimoto, N., Matsuishi, T., Kakuma, T., and Koga, Y.; Taro Matsuoka for MELAS Study Group in Japan. (2012). MELAS: a nationwide prospective cohort study of 96 patients in Japan. Biochim. Biophys. Acta 1820, 619–624.

Yoo, A.S., Sun, A.X., Li, L., Shcheglovitov, A., Portmann, T., Li, Y., Lee-Messer, C., Dolmetsch, R.E., Tsien, R.W., and Crabtree, G.R. (2011). MicroRNA-mediated conversion of human fibroblasts to neurons. Nature 476, 228–231.

Zeviani, M., and Carelli, V. (2007). Mitochondrial disorders. Curr. Opin. Neurol. 20, 564–571.

Address correspondence to: ◀AU12
José A. Sánchez Alcázar
Centro Andaluz de Biología del Desarrollo (CABD)
Consejo Superior de Investigaciones Científicas
Universidad Pablo de Olavide
Carretera de Utrera Km 1
Sevilla 41013
Spain

E-mail: jasanalc@upo.es

AUTHOR QUERY FOR CELL-2022-0055-VER9-POVEACABELLO_1P

AU1: Please note that gene symbols in any article should be formatted as per the gene nomenclature. Thus, please make sure that gene symbols, if any in this article, are italicized.
AU2: Please identify (highlight or circle) all authors' surnames for accurate indexing citations.
AU3: Please confirm the authors' affiliations.
AU4: Include IRB approval or waiver statement in the Materials and Methods section. The Clinical Trial Registration number, if applicable, should be included at the end of the abstract.
AU5: The Publishers request for readability that all paragraphs be limited to 15 typeset lines. Please adjust all paragraphs accordingly.
AU6: Please note that the value ''2.6e4 cells/cm^2'' is given in exponential form in the sentence ''Fibroblasts were plated onto …'' Please check and confirm if this is OK.
AU7: Please expand ''IR-DIC.''
AU8: Please check the spelling is it ''pipette''?
AU9: Please check and confirm whether the ''Author Disclosure Statement'' has been set correctly.
AU10: Please confirm the accuracy of Funding Information.
AU11: References ''Chinnery (2015), El-Hattab et al. (2012), Glover et al. (2010), Gorman et al. (2016), Hamalainen (2014), Inak et al. (2017), Kang et al. (2016), Lekoubou et al. (2011), Lorenz et al. (2017), Ohsawa et al. (2019), Perales-Clemente et al. (2016), Schon et al. (2012), Smith et al. (2015), Zeviani and Carelli (2007)'' are not cited in the text. Please insert the citations in the text.
AU12: Please note that there is mismatch between the corresponding author's address and author's affiliation. Please check.
AU13: Please note that blue squares, red squares, white arrows, yellow arrows, and asterisks are present in the artwork of Figure 1 but not mentioned in the figure legend. Please check.